

RESEARCH ARTICLE

Cytochrome P450 168A1 from *Pseudomonas aeruginosa* is involved in the hydroxylation of biologically relevant fatty acids

Claire L. Price¹, Andrew G. S. Warrilow¹, Nicola J. Rolley¹, Josie E. Parker¹, Vera Thoss², Diane E. Kelly¹, Nicolae Corcionivoschi^{3,4}, Steven L. Kelly^{1*}

1 Centre for Cytochrome P450 Biodiversity, Institute of Life Science, Swansea University Medical School, Swansea University, Swansea, Wales, United Kingdom, **2** Plant Chemistry Group, School of Chemistry, Bangor University, Bangor, Gwynedd, Wales, United Kingdom, **3** Agri-Food and Biosciences Institute, Veterinary Science Division, Bacteriology Branch, Stoney Road, Stormont, Belfast, Northern Ireland, United Kingdom, **4** Faculty of Bioengineering of Animal Resources, Banat University of Agricultural Sciences and Veterinary Medicine, King Michael I of Romania, Timisoara, Romania

* s.l.kelly@swansea.ac.uk



OPEN ACCESS

Citation: Price CL, Warrilow AGS, Rolley NJ, Parker JE, Thoss V, Kelly DE, et al. (2022) Cytochrome P450 168A1 from *Pseudomonas aeruginosa* is involved in the hydroxylation of biologically relevant fatty acids. PLoS ONE 17(3): e0265227. <https://doi.org/10.1371/journal.pone.0265227>

Editor: Alessandro Giuffrè, National Research Council, ITALY

Received: September 11, 2021

Accepted: February 24, 2022

Published: March 21, 2022

Copyright: © 2022 Price et al. This is an open access article distributed under the terms of the [Creative Commons Attribution License](#), which permits unrestricted use, distribution, and reproduction in any medium, provided the original author and source are credited.

Data Availability Statement: All relevant data are within the manuscript and its [Supporting information](#) files.

Funding: This work was supported by the European Union European Regional Development Fund (ERDF) via the Wales European Funding Office of the Welsh Government through the BEACON funding initiative. The funders had no role in study design, data collection and analysis,

Abstract

The cytochrome P450 CYP168A1 from *Pseudomonas aeruginosa* was cloned and expressed in *Escherichia coli* followed by purification and characterization of function. CYP168A1 is a fatty acid hydroxylase that hydroxylates saturated fatty acids, including myristic (0.30 min^{-1}), palmitic (1.61 min^{-1}) and stearic acids (1.24 min^{-1}), at both the ω -1- and ω -2-positions. However, CYP168A1 only hydroxylates unsaturated fatty acids, including palmitoleic (0.38 min^{-1}), oleic (1.28 min^{-1}) and linoleic acids (0.35 min^{-1}), at the ω -1-position. CYP168A1 exhibited a catalytic preference for palmitic, oleic and stearic acids as substrates in keeping with the phosphatidylcholine-rich environment deep in the lung that is colonized by *P. aeruginosa*.

Introduction

Pseudomonas aeruginosa is an opportunistic pathogen, and the leading cause of chronic lung infection in cystic fibrosis patients [1]. *P. aeruginosa* uses the lung surfactant (which is essential for normal breathing, preventing alveoli collapse and acting as a system of lung defense in the lungs) as a source of nutrients allowing it to colonize a large portion of the lungs. This causes airway plugging and surface damage to epithelial cells [1]. The lung surfactant largely consists of a class of phospholipids called phosphatidylcholine. This phospholipid is a source of fatty acids, which are released during degradation by lipases and phospholipases, which are excreted by *P. aeruginosa* [2–4]. These released fatty acids could be broken down through the fatty acid degradation pathway via the β -oxidation cycle [5] to be used as a source of energy or they could be taken up by the cell to be used for other cellular processes.

For instance, upon cellular uptake in other organisms, fatty acids can be metabolized by cytochrome P450 enzymes (CYPs) to produce hydroxy fatty acids, which, in turn, can be used for a variety of physiological functions, including diacid formation [5, 6], sophorolipid

decision to publish, or preparation of the manuscript.

Competing interests: The authors have declared that no competing interests exist.

production [7], and the synthesis of cutin and suberin in plants [8]. While cytochromes P450 (CYPs) are not directly involved in the β -oxidation cycle of fatty acid degradation, they are essential in forming or initiating the formation of hydroxy fatty acids and/or diacids. These molecules can then act as an energy source as they can be degraded by the β -oxidation cycle [5, 6].

It is unlikely, because of their cellular localization, that fatty acid hydroxylating CYPs in *P. aeruginosa* will interact directly with the lung surfactant in order to have access to phosphatidylcholine. Therefore, in order for these CYPs to access the fatty acids released from phosphatidylcholine, *P. aeruginosa* expresses all the relevant genes involved in phosphatidylcholine degradation (lipases: LipA and LipC, and phospholipases: PlcH and PlcR). The expression of these genes results in fatty acids, glycerol and phosphorylcholine being released. The individual constituents are further imported and degraded, via high levels of expression of many genes involved in the fatty acid degradation pathway suggesting that *P. aeruginosa* may utilize phosphatidylcholine as one of the major nutrient sources *in vivo* [2] and could also be made available for interaction with the CYPs.

In this study, we have investigated CYP168A1 from *P. aeruginosa*, the sole member of its cytochrome P450 family, to establish whether this enzyme is able to catalyze the hydroxylation of fatty acids. We have cloned, expressed and purified CYP168A1 and have successfully demonstrated the enzyme's ability to hydroxylate biologically relevant fatty acids at the sub-terminal carbons.

Materials and methods

Chemicals

Growth media, ampicillin, 5-aminolevulinic acid and isopropyl- β -D-thiogalactopyranoside (IPTG) were purchased from Formedium, Ltd. (Hunstanton, UK). Chemicals used in the preparation of phosphate buffers were purchased from Fisher Scientific (Loughborough, UK). Voriconazole was purchased from Discovery Fine Chemicals (Dorset, UK). Palmitoleic acid (C16:1) was purchased from Tokyo Chemical Industry UK Ltd (Oxford, UK). All other fatty acids and chemicals were purchased from Sigma-Aldrich (Poole, UK), unless otherwise stated.

Heterologous expression and purification of CYP168A1 protein

The *CYP168A1* gene (UniProt accession number Q9I107) was synthesized by Eurofins MWG Operon (Ebersberg, Germany) including nucleotide sequence optimization for expression in *E. coli*. The gene was designed to contain the triplet GCT, coding for alanine as the second amino acid, to aid expression in *E. coli* and a C-terminus hexahistidine tag to facilitate purification by affinity chromatography using Ni²⁺-NTA agarose. In addition an *Nde*I restriction site was incorporated at the 5' end and a *Hind*III restriction site at the 3' end of the gene. The gene was cloned using the *Nde*I and *Hind*III restriction sites into pET17b and transformed into BL21(DE3)pLysS cells under ampicillin and chloramphenicol selection. Transformants were used to inoculate Terrific broth containing ampicillin and grown at 37°C and 180 rpm for 6 hours. 1 mM IPTG and 1 mM 5-aminolevulinic acid were added for induction prior to expression. CYP168A1 was expressed at 25°C and 130 rpm for 20 hours. Cells were harvested (10 min at 3000 x g), re-suspended in 0.1 M potassium phosphate buffer (pH 7.4) and stored at -80°C overnight. Samples were thawed and spun at 140000 x g for 1 hour at 4°C to recover the solubilized protein in the supernatant. CYP168A1 was purified using Ni²⁺-NTA agarose (Qiagen) and eluted in 0.1 M Tris-HCl (pH 8.1) containing 25% (w/v) glycerol and 1% (w/v) L-histidine. SDS-polyacrylamide gel electrophoresis was undertaken to assess protein purity.

Determination of cytochrome P450 protein concentration

Reduced carbon monoxide difference spectroscopy was performed (light path, 10 mm) according to the method of Estabrook *et al.*, 1972 [9] to determine cytochrome P450 protein concentration using an extinction coefficient of $91 \text{ mM}^{-1} \text{ cm}^{-1}$ at 450 nm [10]. Absolute spectra were determined from 700 nm to 250 nm (light path, 4.5 mm). The heme concentration of the purified CYP168A1, diluted with 10 mM potassium phosphate (pH 7.4), was determined by measuring the Soret peak at 417 nm using an extinction coefficient of $125 \text{ mM}^{-1} \text{ cm}^{-1}$ [11] and the total protein concentration was determined by measurement of the absorbance at 205 nm using an extinction coefficient of $31 \text{ ml mg}^{-1} \text{ cm}^{-1}$ [12] from which the percentage heme incorporation was calculated. The Reinheitszahl (Rz) ratio of absorbance due to the heme Soret peak at 417 nm and that due to the absorbance of the apoprotein was also determined as a primary indicator of enzyme purity and heme incorporation [13]. All spectral determinations were made using a Hitachi U-3310 UV-visible spectrophotometer (San Jose, CA).

Fatty acid binding studies

Fresh supplies of fatty acids were purchased prior to commencing ligand binding and catalysis studies. Stock solutions containing 0.25 mg ml^{-1} myristic acid (C14:0), palmitic acid (C16:0), stearic acid (C18:0) and oleic acid (C18:1) were prepared in dimethylformamide along with 0.5 mg ml^{-1} palmitoleic acid (C16:1), 0.1 mg ml^{-1} linoleic acid (C18:2) and 10 mg ml^{-1} arachidonic acid (C20:4). These stock fatty acid solutions were progressively titrated against $5 \mu\text{M}$ of CYP168A1 protein in 0.1 M Tris-HCl (pH 8.1) buffer containing 25% (w/v) glycerol using quartz semi-micro cuvettes with equivalent volumes of dimethylformamide added to the cytochrome P450-containing reference cuvette. Titrations of CYP168A1 with myristic (1.09, 2.19, 3.28, 4.38, 5.47, 6.57, 7.66, 8.076 μM), palmitic (0.98, 1.95, 2.93, 3.9, 4.88, 5.83, 6.83, 7.8 μM), stearic (0.88, 1.76, 2.64, 3.52, 4.39, 5.27, 6.15, 7.03 μM), palmitoleic (0.98, 1.97, 2.95, 3.93, 4.91, 5.90, 6.88, 7.86 μM), oleic (0.89, 1.77, 2.66, 3.54, 4.43, 5.31, 6.20, 7.08 μM), linoleic (0.36, 0.71, 1.07, 1.43, 1.78, 2.14, 2.50, 2.85 μM) and arachidonic (33, 66, 99, 132, 165, 198, 231, 264, 297, 330, 363, 396, 429, 462, 495, 528, 561, 594, 627, 660 μM) acids were performed at room temperature.

The absorbance difference spectra from 500 nm to 350 nm were determined after each incremental addition of fatty acid. Ligand saturation curves were constructed from the change in absorbance ($\Delta A_{\text{peak-trough}}$) against fatty acid concentration. The dissociation constant for the fatty acid-CYP168A1 complex (K_s) was determined by nonlinear regression (Levenberg-Marquardt algorithm) using a rearrangement of the Morrison equation [14] and the Michaelis-Menten equation. The magnitude of the spin state change for type I difference spectra was calculated from $\Delta A_{390-420}$ using an extinction coefficient of $100 \text{ mM}^{-1} \text{ cm}^{-1}$ [15]. All fatty acid binding experiments were undertaken in quadruplicate.

In between ligand binding determinations, the quartz cuvettes were washed with deionized water and then soaked for 30 min in 2-propanol at room temperature to desorb any residual fatty acids from the cuvette surfaces, followed by rinsing a further three-times with 2-propanol and then deionized water prior to drying.

Fatty acid reconstitution assays

The reconstitution assay system contained $0.25 \mu\text{M}$ CYP168A1, $2.5 \mu\text{M}$ spinach ferredoxin (Sigma-Aldrich F3013), $0.25 \mu\text{M}$ spinach ferredoxin-NADP⁺ reductase (Sigma-Aldrich F0628), $50 \mu\text{M}$ dilaurylphosphatidylcholine (DLPC), $100 \mu\text{M}$ fatty acid, 4 mM glucose-6-phosphate, 3 U/ml yeast glucose-6-phosphate dehydrogenase and 0.1 M potassium phosphate (pH 7.4). Assay mixtures were incubated at 37°C for 5 min prior to initiation with 4 mM β -

NADPH-Na₄ and then incubated for a further 2.5 hours at the same temperature. Fatty acids and their hydroxylated products were recovered by extraction with dichloromethane and dried in a vacuum centrifuge. TMS derivatisation of the samples and analysis by GCMS were performed as previously described [16]. Percentage product formation was calculated from the GC peak areas of the fatty acid and the hydroxylated metabolites, with compound identities confirmed by mass fragmentation patterns of fatty acid standards.

To test the effect of the azole antifungal drugs miconazole, tebuconazole and voriconazole on CYP168A1 turnover, the reconstitution assays were repeated as described above using oleic acid as the substrate, except 2 μM of azole dissolved in DMF was also present. Control assays contained no azole, but an equivalent volume of DMF. Experiments were undertaken in duplicate.

CYP168A1 reconstitution assays were also performed using 50 μM cholesterol, cholesta-4-ene-3-one, progesterone and testosterone as potential substrates. For these assays the CYP168A1 concentration was increased to 2 μM in the presence of 2.5 μM spinach ferredoxin, 0.25 μM spinach ferredoxin-NADP⁺ reductase, 50 μM DLPC, 4 mM glucose-6-phosphate, 3 U/ml yeast glucose-6-phosphate dehydrogenase, 0.1 M potassium phosphate (pH 7.4) and 4 mM β-NADPH-Na₄, followed by 3 hours incubation at 37°C. Steroid and sterol compounds were extracted with ethyl acetate (2 x 3 ml), dried using a vacuum centrifuge and derivatized firstly with methoxamine followed by silylation using BSTFA-TMCS and analyzed by GCMS (57). Metabolites were identified from GC traces and MS fragmentation patterns compared against positive controls for CYP mediated hydroxylation reactions performed in our laboratory.

Azole binding studies

The azole antifungal drugs miconazole, tebuconazole and voriconazole were used in binding studies with CYP168A1 in accordance with previously described methods [17, 18]. Stock solutions of these azoles (0.75–10 mg ml⁻¹) were prepared in DMF and progressively titrated against 2 μM CYP168A1 in 0.1 M Tris-HCl (pH 8.1) buffer containing 25% (w/v) glycerol. Equivalent volumes of DMF were added to a reference cuvette containing 2 μM of CYP168A1. Titrations with miconazole (1.80, 3.60, 5.41, 7.21, 9.01, 10.81, 12.61 μM), tebuconazole (16.24, 32.49, 48.73, 64.97, 81.22, 97.46, 113.70 μM) and voriconazole (28.63, 57.26, 85.88, 114.51, 143.14, 171.77, 200.40, 229.02, 257.65 μM) were performed at room temperature.

The difference spectrum from 500 nm to 350 nm was determined after each incremental addition of azole. Binding saturation curves were constructed from the ΔA_{peak-trough} against azole concentration. The dissociation constant (K_d) of the enzyme-azole complex was determined by nonlinear regression (Levenberg-Marquardt algorithm) using a rearrangement of the Morrison equation [14]. All binding experiments were undertaken in duplicate.

MIC determinations

P. aeruginosa strains DSMZ 22644 and ATCC 39324 were grown in LB media overnight. Optical density at 520 nm of the overnight cultures was measured using a spectrophotometer. Cultures were adjusted to give an optical density of approximately 0.2, which is equivalent to a cell count of approximately 1 x 10⁹. The cells were pelleted and resuspended in the same volume of water. Further dilutions were made in M9 media with oleic acid used as the carbon source (instead of glucose) to give approximately 2 x 10⁵ cells. Stock concentrations of tebuconazole, miconazole and voriconazole were prepared in dimethyl sulfoxide (12.8, 6.4, 3.2, 1.6, 0.8, 0.4, 0.2, 0.1, 0.05 and 0.025 mg ml⁻¹). These stock azole solutions were diluted ten-fold in fresh LB media and then diluted a further ten-fold with inoculum in microtiter plate wells. This gave

final azole concentrations of 128, 64, 32, 16, 8, 4, 2, 1, 0.5 and 0.25 $\mu\text{g ml}^{-1}$. The microtiter plates were incubated at 37°C for 24 hours. Following this initial incubation period, 20 μl of 0.2% Resazurin was added to each microtiter plate well. The plates were incubated for a further 48 hours at 37°C before being read. A color change from purple to pink indicated the presence of respiring cells. Each azole MIC determinations were performed in triplicate and scored manually.

Data analysis

Curve-fitting of ligand binding data were performed using the computer program QuantumSoft ProFit (version 6.1.12). Phylogenetic analysis of CYP168A1 was performed using the UniProt BLAST online software resource (<http://www.uniprot.org/blast/>). Amino acid sequence alignments were performed using ClustalX version 1.81 software (<http://www.clustal.org/>).

Results

Heterologous expression of CYP168A1

Overexpression of CYP168A1 in *E. coli* resulted in protein yields of ~900 nmol per liter of culture. SDS-polyacrylamide gel electrophoresis, following Ni^{2+} -NTA agarose purification, confirmed that CYP168A1 was over 90% pure as judged by staining intensity with Coomassie brilliant blue R-250. The absolute spectrum of CYP168A1 (Fig 1A) was characteristic of a ferric cytochrome P450 enzyme that had been isolated predominately in the low-spin state with a Soret peak at 417 nm [19, 20]. The $A_{393-470}/A_{417-470}$ value was 0.412, where 0.4 is indicative of 100% low-spin occupancy and 2.0 indicative of 100% high-spin occupancy [21], confirming CYP168A1 to be over 95% low-spin in the oxidized resting state. The observed A_{417}/A_{280} for CYP168A1 was 1.26, which was within the expected range of 1 and 2 for a cytochrome P450 [13]. Heme incorporation was 77 to 81% calculated from measurements at A_{205} and A_{417} [11, 12] with a specific heme content of 15.3 nmol mg^{-1} protein comparable to the expected value of 17 to 20 nmol mg^{-1} for cytochrome P450 enzymes [13]. The dithionite-reduced carbon monoxide difference spectrum for CYP168A1 (Fig 1B) was characteristic of CYPs isolated in their native state exhibiting a red-shifted Soret peak at 450 nm [9, 10].

Phylogenetic analysis of CYP168A1

P. aeruginosa strain PAO1 contains three putative cytochrome P450 monooxygenases PA2475, PA3331 and PA3679 (<https://www.pseudomonas.com/>) and these have been assigned as CYP168A1, CYP107S1 and CYP169A1 (<https://drnelson.uthsc.edu/>) with corresponding UniProt accession numbers Q9I107, Q9HYR4 and Q9HXW1, respectively.

Phylogenetic analysis using BLASTP indicated CYP168A1 to be confined to *Acinetobacter baumannii*, *Enterobacter cloacae* and *P. aeruginosa* (sequence identities 98.2 to 99.8%) with some genes putatively described as 'biotin biosynthesis cytochrome P450 bioI'. The latter 'bioI' genes included *A. baumannii* UniProt accession number A0A1G5LRV6 (99.8% sequence identity) and *P. aeruginosa* A0A0P1DBG8 and A0A0F7QM08 (both 99.8% sequence identities). Sequence identity falls to 35–42% for the next closest group of cytochrome P450 enzymes, which feature numerous CYPs from *Streptomyces* sp., and CYPs from *Candidatus Rokubacteria bacterium*, *Allokutzneria albata*, *Microcystis aeruginosa*, *Scytonema hofmannii*, *Amycolatopsis orientalis*, *Saccharomonospora cyanea*, *Nitrolancea hollandica*, *Actinomadura madurae*, *Kutzneria albida*, and *Actinobacteria bacterium*. Nearly all of these CYPs were of unknown function, but some were assigned putative functions of Linalool 8-monooxygenase, CYP107B1, and peroxidase enzymes. Alignment of the CYP168A1 amino acid sequence

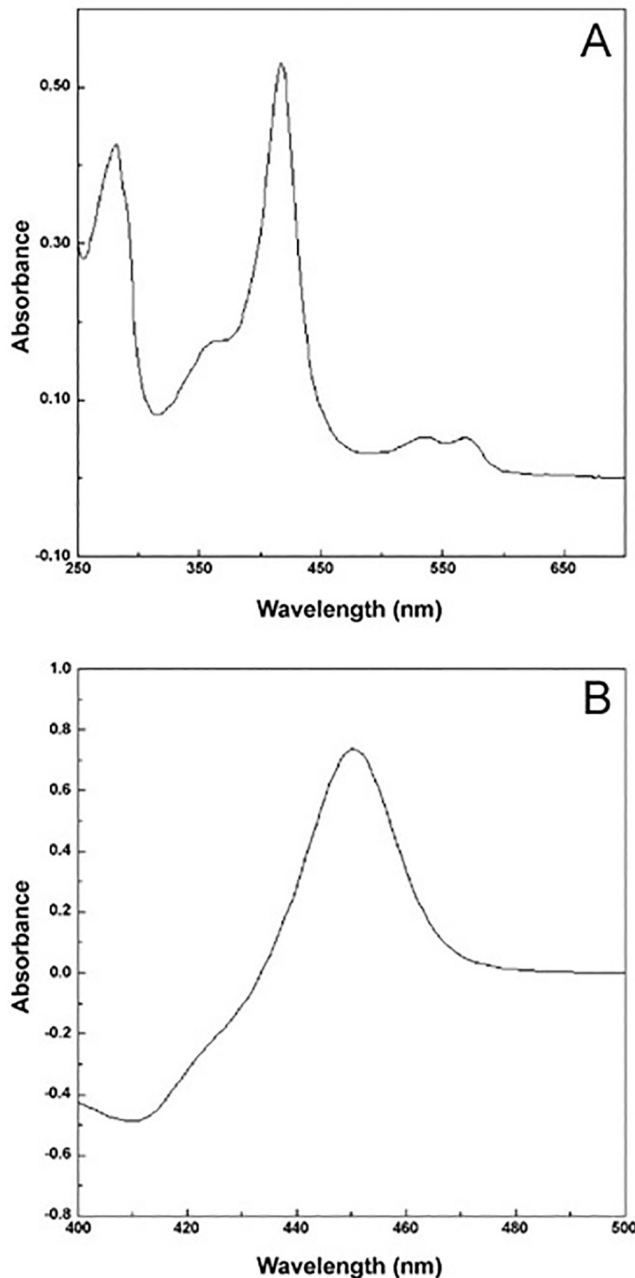


Fig 1. Spectral properties of CYP168A1. The absolute spectrum of a twenty-fold dilution of purified CYP168A1 in the oxidized resting state (4.5 mm light path) is shown (A) in addition to the dithionite-reduced carbon monoxide difference spectrum (light path 10 mm) of 9 μ M purified CYP168A1 (B).

<https://doi.org/10.1371/journal.pone.0265227.g001>

against CYP107H1 enzymes from *Bacillus subtilis* (P53554), *Bacillus amyloliquefaciens* (Q70JZ2) and *Bacillus licheniformis* (Q65MK8) showed that only 9 out of the 32 residues associated with CYP107H1 function in *Bacillus sp.* [22] were also conserved in CYP168A1 (excluding the heme-coordinating cysteine residue) and that CYP168A1 shared only 31% sequence identity with the *Bacillus* CYP107H1 enzymes. Therefore, CYP168A1 did not appear to be a CYP107H homolog.

Fatty acids are able to bind to CYP168A1

The heme prosthetic group of CYPs exists in equilibrium between the low-spin (hexacoordinate) form, characterized by a heme Soret peak at ~418 nm, and the high-spin (pentacoordinate) form, characterized by a heme Soret peak at ~393 nm. The resting state of most CYPs is predominantly the low-spin ferric form [23]. Ligand binding can perturb the spin state equilibrium in two main ways. Substrates and other ligands can bind to the CYP (though the ligands themselves do not directly coordinate to the heme) resulting in the displacement of the axial-ligated water molecule from the heme ferric ion and a change in spin state from low- to high-spin. The magnitude of the spin state change observed is dependent on both the CYP and the ligand. For example, lauric acid binding to *Streptomyces peucetius* CYP147F1 causes 95% of the enzyme molecules to undergo a low- to high-spin state transition [24], whereas for eukaryotic CYP51 enzymes the spin state changes associated with substrate binding rarely exceed 10% [25]. This low- to high-spin transition gives rise to a type I difference spectrum that is characterized by a spectral peak at ~390 nm and trough at ~420 nm. Other ligands can directly coordinate to the heme ferric ion (commonly through an aromatic nitrogen atom) [19, 26], for example the binding of azole antifungals to CYP51 enzymes [27]. The resultant complexes are low-spin (hexacoordinate) and often result in a red-shift of the Soret peak from 418 nm to 425–434 nm [19]. This direct coordination of the ligand to the heme ferric ion gives rise to a type II difference spectrum [19]. The spectral peak varies from 425 nm (if the CYP was 100% in the high-spin state before ligand binding) to 432 nm (if the CYP was 100% in the low-spin state) with respective troughs of 390 nm and 410 nm. For CYPs of mixed spin state the peaks and troughs will be at intermediate wavelengths.

Type I absorption difference spectra were obtained for all the fatty acids with 5 μM CYP168A1. The peak at 393 nm and trough at 418 nm is most clearly shown for the difference spectrum obtained with 0.5 μg ml⁻¹ fatty acid and 5 μM CYP168A1 (Fig 2), equivalent to 2.19, 1.95, 1.76, 1.97, 1.77 and 1.78 μM for myristic, palmitic, stearic, palmitoleic, oleic and linoleic acid, respectfully. The cumulative difference spectra obtained during the ligand titration for myristic acid (C14:0), palmitic acid (C16:0), palmitoleic acid (C16:1), stearic acid (C18:0), oleic acid (C18:1), and linoleic acid (C18:2) and the associated ligand saturation curves are shown in Figs 3 and 4 for arachidonic acid (C20:4). These type I difference spectra suggest that all seven fatty acids were potential substrates for CYP168A1. Spectral isosbestic points were observed for palmitic (404 nm), stearic (404 nm), palmitoleic (406 nm), oleic (403 nm) and linoleic (406 nm) acids. However, no clear isosbestic points were observed for myristic and arachidonic acids due to the spectral peak at ~393 nm progressively diminishing above a threshold fatty acid concentration whilst the spectral trough at ~421 nm continued to deepen.

It was important to optimize the stock fatty acid concentrations so as to obtain sufficient ascendant points on the titration curve before reaching ligand saturation to facilitate curve fitting of data and accurate K_s determination, especially as the type I difference spectra for some fatty acids (notably stearic, palmitoleic and oleic acids) started to dissipate at higher ligand concentrations (Fig 3). This may be caused by either slow aggregation of the CYP168A1-fatty acid complex (although no visible precipitation was observed) or a perturbation of the spin-state equilibrium of the CYP168A1-substrate complex so that some molecules transition to the low-spin state by partial coordination of a water molecule as the sixth axial heme ligand. This phenomenon was evident in the ligand saturation curve for palmitic acid with CYP168A1 reported by Tooker et al [28].

This phenomenon of partial dissipation of type I binding spectra at higher ligand concentrations had previously been observed for cholesterol (but not 4-cholest-3-one) binding to CYP125 from *Mycobacterium tuberculosis* [29]. Capyk et al [29] demonstrated this

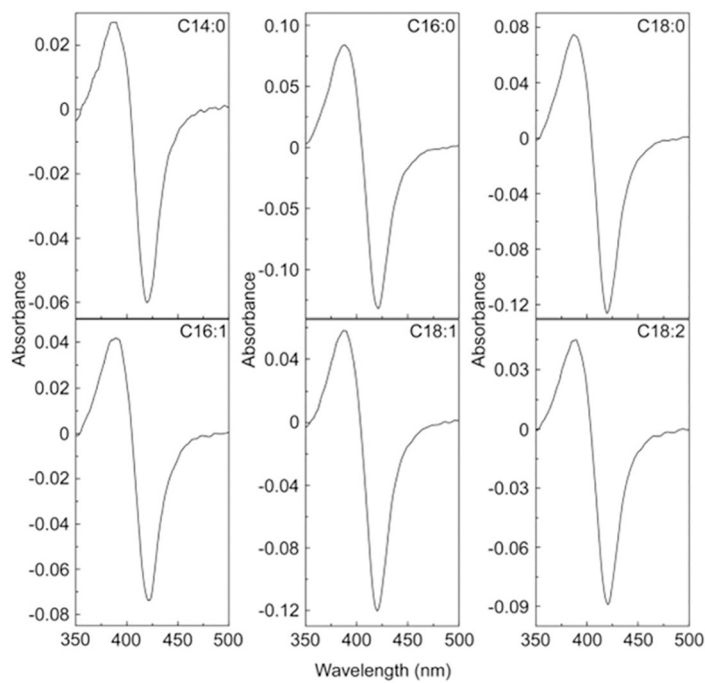


Fig 2. Type i absorbance difference spectra. Absorbance difference spectra were determined using $0.5 \mu\text{g ml}^{-1}$ myristic (C14:0), palmitic (C16:0), stearic (C18:0), palmitoleic (C16:1), oleic (C18:1) and linoleic (C18:2) acids and $5 \mu\text{M}$ CYP168A1 in quartz semi-micro cuvettes of 10 mm path length at room temperature. Composite type I difference spectra and saturation curves for the titration of each fatty acid can be found in Fig 3.

<https://doi.org/10.1371/journal.pone.0265227.g002>

phenomenon was due to the ligand solvent (10% w/v 2-hydroxypropyl- β -cyclodextrin), as when the solvent was changed (to 25 mM EDTA-bridged β -cyclodextrin dimer) the premature dissipation of the type I difference spectrum was no longer observed with cholesterol. As the partial dissipation of type I binding spectra appears to be both ligand- and solvent-specific, both molecules must interact with the CYP protein to cause this effect. When the fatty acid solvent was changed from DMF to ethanol the partial dissipation of the type I binding spectra still occurred at higher ligand concentrations.

The binding saturation curves for all the fatty acids, except arachidonic acid, were best fit using a rearrangement of the Morrison equation [14] (Table 1, Fig 3) to calculate the dissociation constant of the substrate-CYP168A1 complex (K_s), indicating tight binding to CYP168A1. The Michaelis-Menten equation gave the best fit for arachidonic acid binding (Fig 4). Stearic and linoleic acids bound the tightest to CYP168A1 with apparent K_s values under $0.05 \mu\text{M}$, followed by palmitic acid ($K_s 0.12 \mu\text{M}$), then oleic and palmitoleic acids ($K_s \sim 0.15 \mu\text{M}$) and myristic acid ($K_s 0.25 \mu\text{M}$), with arachidonic acid binding having the lowest affinity ($K_s \sim 460 \mu\text{M}$). The fold-difference in apparent K_s values compared to stearic and linoleic acids were ~ 2 -, ~ 3 -, ~ 3 -, ~ 5 -, and ~ 9160 -fold for palmitic, oleic, palmitoleic, myristic, and arachidonic acids, respectively. The high K_s value for arachidonic acid suggested it would be a poor CYP168A1 substrate. Therefore, based on apparent ligand binding affinities, CYP168A1 exhibits a preference for C16 to C18 fatty acids. The magnitude of the low- to high-spin transitions induced were 23, 58, 37, 66, 55, 28 and 32% for myristic, palmitic, palmitoleic, stearic, oleic, linoleic and arachidonic acids, respectively, based on the observed ΔA_{\max} values (Table 1).

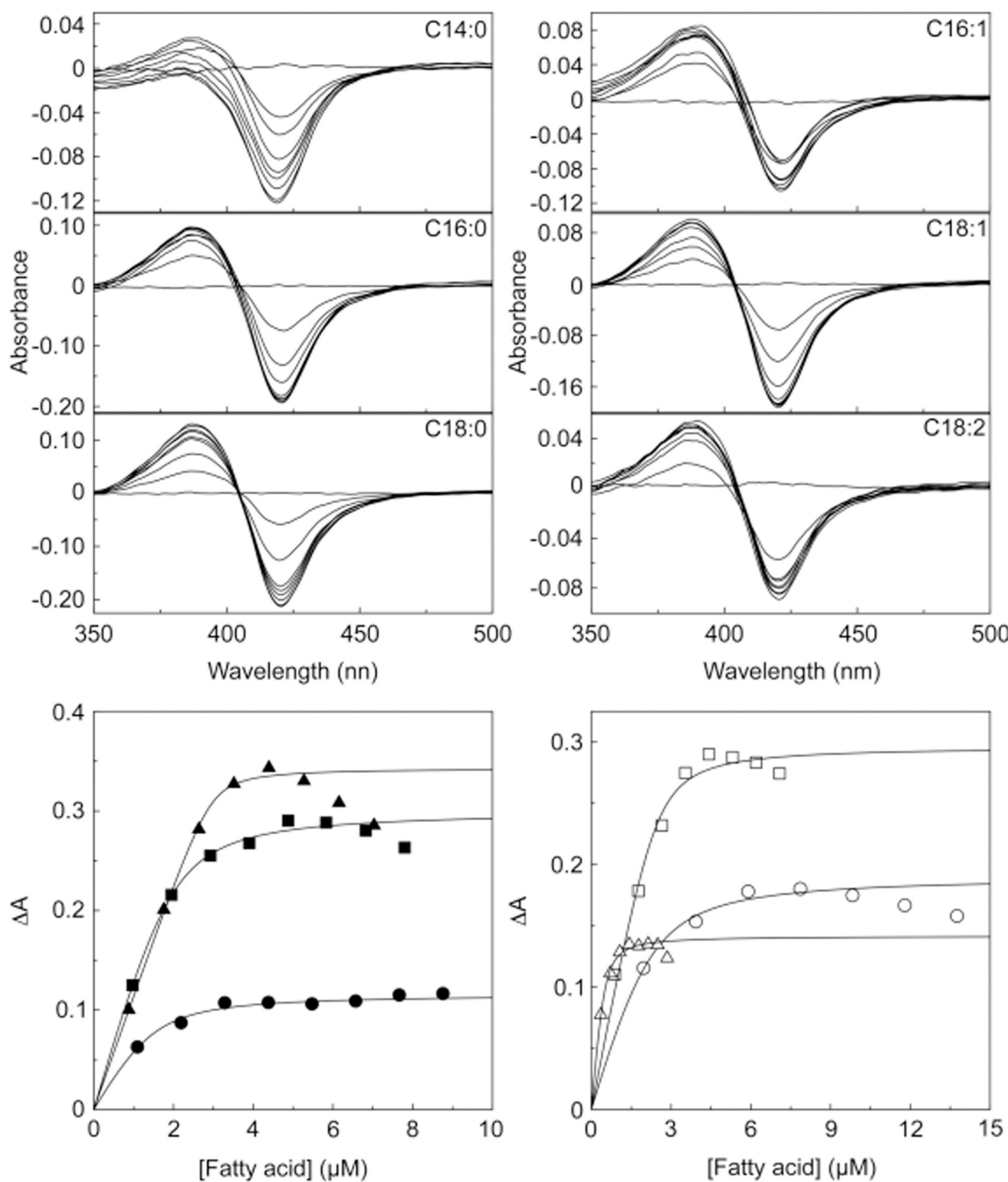


Fig 3. Fatty acid binding to CYP168A1. Myristic, palmitic, stearic and oleic acids (0.25 mg ml^{-1} in DMF), palmitoleic acid (0.5 mg ml^{-1} in DMF) and linoleic acid (0.1 mg ml^{-1} in DMF) were progressively titrated against $5 \mu\text{M}$ CYP168A1 in quartz semi-micro cuvettes of path length 10 mm. After each $1 \mu\text{l}$ addition of fatty acid the difference spectrum was measured against a CYP168A1-containing reference cuvette in which an equivalent volume of DMF was added. Ligand saturation curves for myristic (filled circles), palmitic (filled squares), stearic (filled triangles), palmitoleic (empty circles), oleic (empty squares) and linoleic (empty triangles) acids were constructed and fitted using a rearrangement of the Morrison equation [14]. Ligand binding experiments were performed in quadruplicate, although only one replicate is shown.

<https://doi.org/10.1371/journal.pone.0265227.g003>

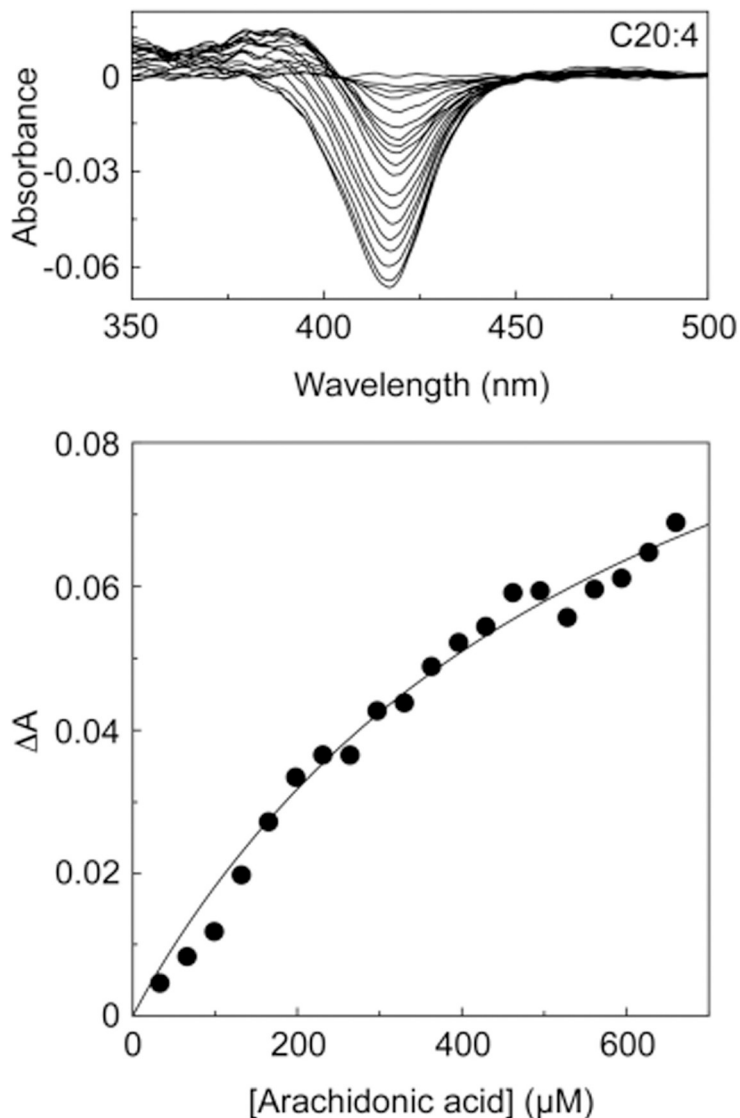


Fig 4. Arachidonic acid binding to CYP168A1. Arachidonic acid (10 mg ml^{-1} in DMF) was progressively titrated against $5 \mu\text{M}$ CYP168A1 in quartz semi-micro cuvettes of path length 4.5 mm. After each $1 \mu\text{l}$ addition of arachidonic acid the difference spectrum was measured against a CYP168A1-containing reference cuvette in which an equivalent volume of DMF was added. The ligand saturation curve was constructed and fitted using the Michaelis-Menten equation.

<https://doi.org/10.1371/journal.pone.0265227.g004>

CYP168A1 preferentially hydroxylates fatty acids at the ω -1 carbon

CYP168A1 was able to catalyze the hydroxylation of the saturated fatty acids myristic acid, palmitic acid, and stearic acid at both the ω -1- and ω -2-carbons (Fig 5A and 5B), showing preference for the ω -1-carbon (Table 2). In this assay system, CYP168A1 gave the highest catalytic turnover with palmitic acid resulting in the formation of ω -1 hydroxypalmitic acid at 1.27 min^{-1} and ω -2 hydroxypalmitic acid at 0.34 min^{-1} (Fig 5C; Table 2). Using palmitic acid as substrate resulted in 4.7- and 1.2-fold more ω -1-hydroxy product and 10.3- and 2-fold more ω -2-hydroxy product being formed than when myristic acid and stearic acid were used, respectively (Table 2). However, the proportion of myristic acid converted to ω -1-hydroxy product

Table 1. Fatty acid binding affinities for CYP168A1.

Fatty acid	K_s (μM)	ΔA_{\max}	Low- to high-spin state change (%)
Myristic acid	0.249 ± 0.103	0.144 ± 0.08	22.8 ± 1.6
Palmitic acid	0.117 ± 0.056	0.290 ± 0.015	58.1 ± 3.0
Palmitoleic acid	0.155 ± 0.083	0.185 ± 0.006	37.0 ± 1.2
Stearic acid	$<0.05^{\text{a}}$	0.328 ± 0.020	65.6 ± 4.1
Oleic acid	0.142 ± 0.012	0.277 ± 0.014	55.4 ± 2.8
Linoleic acid	$<0.05^{\text{a}}$	0.142 ± 0.013	28.3 ± 2.6
Arachidonic acid	458 ± 87	$0.071 \pm 0.009^{\text{b}}$	$31.6 \pm 4.0^{\text{b}}$

Type I difference spectra were observed for all seven fatty acids with 5 μM CYP168A1.

Mean K_s values from four replicates were calculated using a rearrangement of the Morrison equation [14] and are shown \pm standard deviations, except for arachidonic acid where the Michaelis-Menten equation was used.

^a The K_s values for these two fatty acids were below the lower accuracy limit of the Morrison equation of 0.05 μM (1% the concentration of the enzyme) [61].

^b Path length of cuvettes used with arachidonic acid were 4.5 mm compared to 10 mm used with the other fatty acids. Binding saturation was not achieved at 660 μM arachidonic acid.

<https://doi.org/10.1371/journal.pone.0265227.t001>

than ω -2-hydroxy product was substantially higher than observed for the other two saturated fatty acids. The mass fragmentation patterns of the CYP168A1 metabolites ω -1-hydroxypalmitic, ω -2-hydroxypalmitic and ω -1-hydroxyoleic acids are shown in S1 Fig. The mass fragmentation patterns for the TMS-derivatised fatty acid standards can be found in the publication by Williams et al. [30].

CYP168A1 was also able to hydroxylate the unsaturated fatty acids palmitoleic acid, oleic acid and linoleic acid, but only at the ω -1-carbon. Catalytic turnover with oleic acid was similar to that of palmitic acid in terms of production of the ω -1-hydroxy metabolite ω -1-hydroxyoleic acid (1.28 min^{-1}) (Fig 5D, Table 2) and was 3.4- and 3.7-fold greater than the relative ω -1-hydroxy metabolites produced when palmitoleic and linoleic acids were used as substrates. Lower catalytic turnovers were observed with palmitoleic and linoleic acids (0.38 and 0.35 min^{-1} , respectively) although both these fatty acids bound tightly to CYP168A1 (K_s values of $0.155 \mu\text{M}$ and $>0.05 \mu\text{M}$, respectively). Reconstitution assays with arachidonic acid showed no detectable product formation and a large K_s value of $458 \mu\text{M}$ was obtained for arachidonic acid with CYP168A1 (Table 1). No C-C cleavage of fatty acyl chains was detected in the assay products, suggesting that CYP168A1 was not a CYP107H homolog.

Catalytic turnover established the order of substrate preference to be palmitic acid (highest turnover) followed by oleic acid, stearic acid, palmitoleic acid, linoleic acid and finally myristic acid with the lowest turnover (5.3-fold lower than palmitic), whilst arachidonic acid was catalytically inactive. In contrast, the fatty acid K_s data suggested the order of substrate preference would have been stearic and linoleic acids, with the lowest K_s values, followed by oleic acid, palmitoleic acid, myristic acid, and finally arachidonic acid with a 9000-fold larger K_s value than stearic acid. Both stearic and linoleic acids gave similar apparent K_s values with CYP168A1 and yet the catalytic turnover observed with stearic acid was 3.5-fold greater than that for linoleic acid. Further investigations are required in order to determine the mechanisms responsible for the observed differences in CYP168A1 catalytic turnover between substrates.

CYP168A1 reconstitution assays using cholesterol, cholesta-4-ene-3-one, progesterone and testosterone as potential substrates gave no oxygenated products, suggesting CYP168A1 is a fatty acyl hydroxylase.

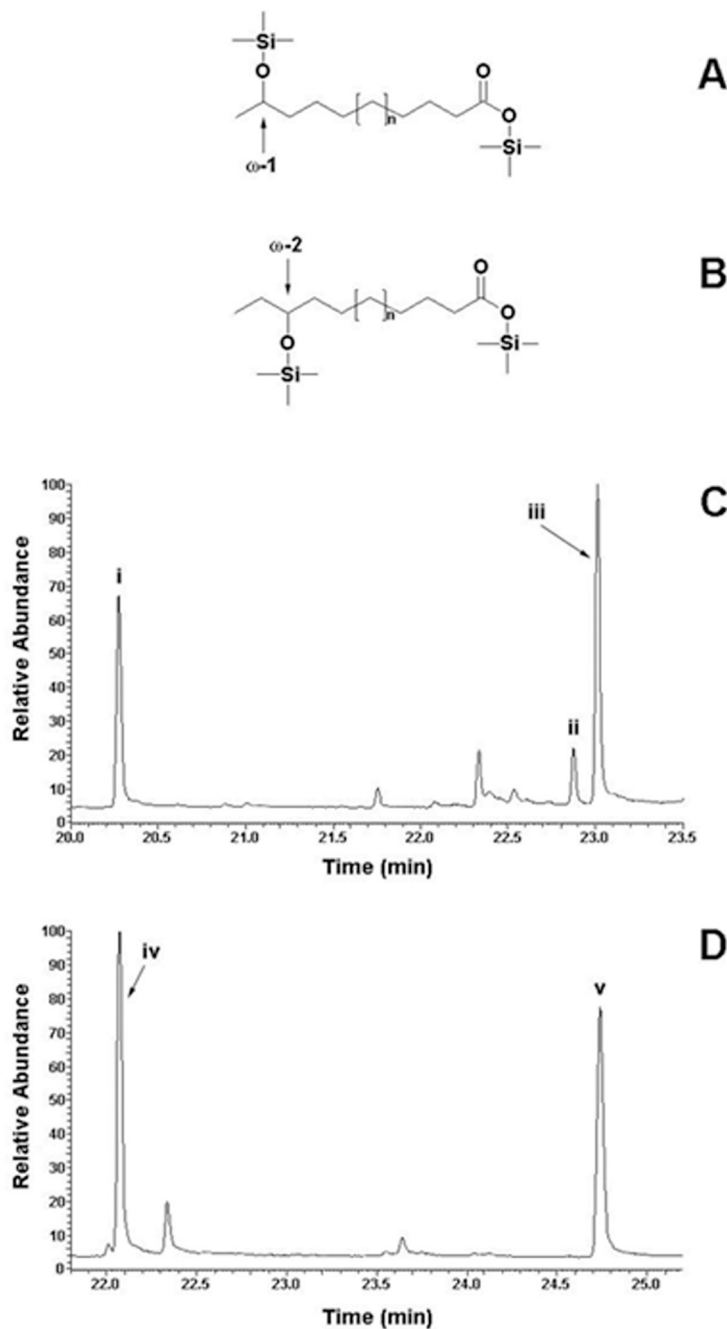


Fig 5. Gas chromatograms of CYP168A1 assay metabolites. The chemical structures of TMS-derivatised ω -1-hydroxy fatty acids (A) and ω -2-hydroxy fatty acids (B) are shown. Gas chromatograms for TMS-derivatized assay metabolites obtained when palmitic acid (C) and oleic acid (D) were used as substrates are shown. Peak (i) corresponds to palmitic acid, peak (ii) to ω -2-hydroxypalmitic acid, peak (iii) to ω -1-hydroxypalmitic acid, peak (iv) to oleic acid and peak (v) to ω -1-hydroxyoleic acid (all TMS-derivatives). Mass fragmentation patterns of the palmitic acid products can be found in the supporting information ([S1 Fig](#)). Other minor GC peaks were identified as impurities present in the source fatty acids.

<https://doi.org/10.1371/journal.pone.0265227.g005>

Table 2. Fatty acid hydroxylation by CYP168A1.

Fatty acid	Carbon hydroxylated	% Product ^a	Turnover no. (min ⁻¹)
Myristic acid	ω-1-	11 ± 0.6	0.27 ± 0.02
	ω-2-	1.3 ± 0.03	0.033 ± 0.001
Palmitic acid	ω-1-	49 ± 3.8	1.27 ± 0.10
	ω-2-	13 ± 4.0	0.34 ± 0.10
Palmitoleic acid	ω-1-	15 ± 2.4	0.38 ± 0.06
	ω-2-	-	-
Stearic acid	ω-1-	41 ± 2.9	1.07 ± 0.09
	ω-2-	6.6 ± 0.5	0.17 ± 0.01
Oleic acid	ω-1-	49 ± 1.2	1.28 ± 0.03
	ω-2-	-	-
Linoleic acid	ω-1-	14 ± 1.3	0.35 ± 0.03
	ω-2-	-	-

Mean values from two replicates ± standard error are presented.

^a percentage of substrate converted into hydroxylated product after 2.5 h incubation at 37°C. The starting substrate and CYP168A1 concentrations were 100 μM and 0.25 μM, respectively. No hydroxylated products were obtained when 100 μM arachidonic acid was used as substrate.

<https://doi.org/10.1371/journal.pone.0265227.t002>

Azoles are able to bind to CYP168A1, but they have no effect on *P. aeruginosa* growth

CYP168A1 was titrated against the azole antifungal drugs tebuconazole, voriconazole and miconazole. The enzyme was able to bind each of the three azoles, eliciting type II difference spectra (Fig 6), with apparent dissociation constants (K_d) for the azole-CYP168A1 complexes of 0.18 ± 0.01 , 2.05 ± 0.54 and 0.19 ± 0.06 μM for tebuconazole, voriconazole and miconazole,

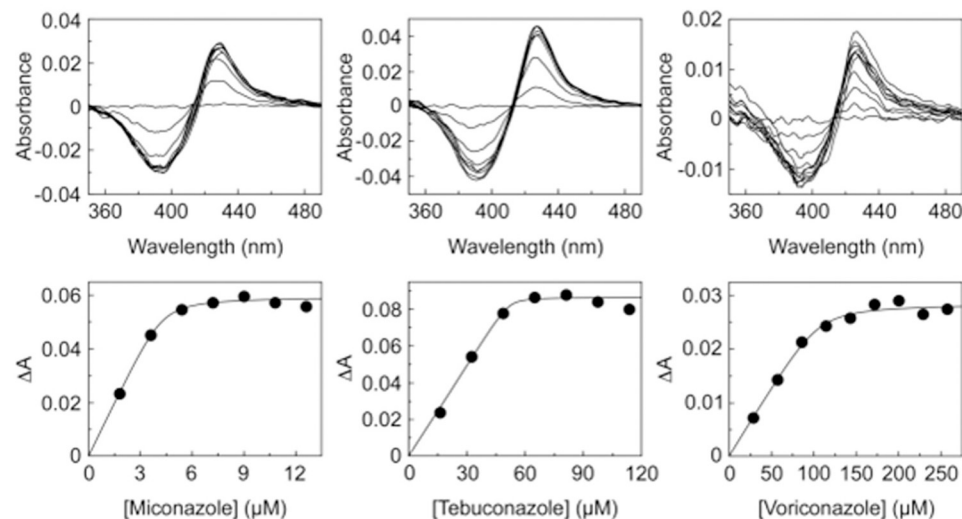


Fig 6. Binding of azole antifungals to CYP168A1. Miconazole (0.75 mg ml⁻¹), tebuconazole (5 mg ml⁻¹) and voriconazole (10 mg ml⁻¹) were progressively titrated against 2 μM CYP168A1 in quartz semi-micro cuvettes of path length 4.5 mm. After each 1 μl addition of azole solution the difference spectrum was measured against a CYP168A1-containing reference cuvette in which an equivalent volume of DMF was added. The cumulative type II difference spectra are shown along with the ligand saturation curves which were fitted using a rearrangement of the Morrison equation [14].

<https://doi.org/10.1371/journal.pone.0265227.g006>

respectively, calculated from the ligand saturation curves (Fig 6). This was in contrast to K_d values for tebuconazole, voriconazole and miconazole obtained with *Candida albicans* CYP51 of 0.036, 0.010 and 0.026 μM , respectively [27, 31]. The addition of 2 μM azoles to reconstitution assays containing 0.25 μM CYP168A1 showed they elicited no effect on the catalytic activity towards oleic acid when compared against the DMF control. However, the presence of 0.5% DMF in the CYP168A1 assay system caused a 10-fold reduction in oleic acid turnover.

Tebuconazole, voriconazole and miconazole were used in minimum inhibitory concentration (MIC) determinations with *P. aeruginosa* strains DMZ 22644 and ATCC 39324 grown on oleic acid. In all cases, the azoles at concentrations up to 128 $\mu\text{g ml}^{-1}$ had no inhibitory effect on *P. aeruginosa* growth as the Resazurin indicator turned pink in all wells, indicating cell respiration.

Discussion

Fatty acids are essential for cell life. Hydroxylation of these molecules can result in the formation of hydroxy fatty acids that can act as signaling molecules and can be used to produce more complex molecules, such as diacids [7, 32]. Therefore, identification and characterization of enzymes involved in fatty acid metabolism is important, particularly in pathogens, such as *P. aeruginosa*, where insight into their function can be used to identify new potential targets for novel inhibitors and teach us more about the mechanism of fatty acid degradation.

CYP168A1 was able to bind a range of biologically relevant fatty acids. The K_s range of <0.05 to 0.25 μM for fatty acids that were catalytically active with CYP168A1 were similar to those observed previously for *Streptomyces peucetius* CYP147F1 [24], *Sorangium cellulosum* CYP267A1 [33], *Streptomyces coelicolor* A3(2) CYP105D5 [34], and some studies with *Bacillus megaterium* CYP102A1 [35]. The K_s values in this study were similar to those recently reported for *P. aeruginosa* CYP168A1 [28], with the exception for stearic acid which was over 6-fold lower (<0.05 μM compared to 0.327 μM) and arachidonic acid which was over 400-fold higher (458 μM compared to 0.96 μM) with the latter mainly due to the atypical difference spectrum observed with arachidonic acid in this study. Higher K_s values have been observed (8 to 30 μM) with *Bacillus subtilis* CYP107H1 [36] and substantially higher K_s values (19 to 1065 μM) observed with *Bacillus subtilis* CYP102A2 and CYP102A3 [37].

CYP168A1 fatty acid turnover rates were similar to those obtained with *Sphingomonas paucimobilis* CYP152B1 [38], with both CYPs giving highest turnovers with palmitic acid, and with *Sorangium cellulosum* CYP267A1 [33], except the highest turnover was obtained for capric acid with CYP267A1. Fatty acid turnover rates with CYP168A1 were ~10-fold higher than those observed with *Mycobacterium marinum* CYP153A16 and *Marinobacter aquaeolei* CYP153A [39] and turnover of palmitic acid was 23-fold greater than observed with *Mycobacterium tuberculosis* CYP124 [40]. The CYP168A1 turnover numbers obtained in this study, although being relatively low for cytochrome P450 monooxygenases, were similar to those reported by Tooker et al [28] of 0.138 min^{-1} with lauric acid and 0.222 min^{-1} with arachidonic acid, however, in this study no catalytic activity was observed with arachidonic acid. At present we cannot account for this difference, although solubility / bioavailability of arachidonic acid in the in vitro reconstitution assay may be a contributory factor. Interestingly, Tooker et al [28] CYP168A1 K_m for lauric acid was 25-fold higher than the K_s value, suggesting that other parameters besides substrate binding affinity were significant contributors to the observed K_m value.

In contrast, CYP168A1 fatty acid turnovers were 10- to 30-fold lower than observed with *Streptomyces peucetius* CYP147F1 [24] and *Candida albicans* CYP52A21 [41], and 25- to 10000-fold lower than observed with *Bacillus subtilis* CYP102A2 and CYP102A3 [37],

Fusarium oxysporum CYP505 [42], and *Bacillus megaterium* CYP102A1 [35]. *S. coelicolor* CYP105D5 fatty acid turnover was greatest with lauric, oleic and arachidonic acids, but gave low turnovers with myristic and palmitic acids [34]. In contrast CYP168A1 exhibited greatest turnover with palmitic, stearic and oleic acids. Therefore, CYP168A1 fatty acid turnover rates were similar to some bacterial CYP fatty acid hydroxylases but are substantially lower than others, especially the CYP102 family, and are 50- to 100-fold lower than the rates of lauric acid hydroxylation observed with human CYP4A1 and CYP4A3 [43, 44].

CYP168A1 from *P. aeruginosa* is able to hydroxylate biologically relevant saturated fatty acids at both the ω -1- and ω -2-positions, while it can only hydroxylate unsaturated fatty acids at the ω -1-position. Fatty acid terminal and sub-terminal hydroxylating CYPs from other bacteria tend to be able to hydroxylate fatty acids at a wider range of positions. For instance, CYP107H1 from *Bacillus subtilis* has been shown to hydroxylate myristic acid at the ω -1-, ω -2- and ω -3-carbons, and at the ω -1-, ω -2-, ω -3-, ω -4- and ω -5-carbons in palmitic acid [45]. Interestingly, CYP107H1 preferentially hydroxylates myristic acid at the ω -3-carbon and showed similar hydroxylation at all 5 positions noted in palmitic acid [45], whereas CYP168A1 was shown to preferentially hydroxylate at the ω -1-position regardless of chain length. The inability of CYP168A1 to metabolize cholesterol, cholesta-4-ene-3-one, progesterone and testosterone suggests the enzyme is a fatty acyl hydroxylase.

Not all bacterial fatty acid hydroxylating CYPs only hydroxylate unsaturated fatty acids at one position. For instance, CYP105D5 can hydroxylate oleic acid at multiple positions with a preference for the ω -1-position [34]. CYP102A1 can also cause the epoxidation of unsaturated fatty acids, but no epoxidation was observed when CYP168A1 was used in reconstitution assays with unsaturated fatty acids, such as oleic acid and linoleic acid. In the presence of arachidonic acid, CYP102A1 is able to both hydroxylate at the ω -2-carbon and cause epoxidation between carbons 14 and 15 [46], whereas CYP168A1 showed no turnover of arachidonic acid in this study.

In all cases, CYP168A1 was only able to hydroxylate the fatty acids at the sub-terminal carbons, with no activity observed at the terminal, ω - carbon, unlike other bacterial fatty acid hydroxylating CYPs, such as CYP124 (36) and CYP119 from *Sulfolobus acidocaldarius* [47], and those from eukaryotes, such as members of the CYP52 family in yeast [32, 41] and the CYP4 family in mammals [48–51]. Therefore, CYP168A1 is unlikely to be involved in the production of α,ω -diacids. In order to hydroxylate fatty acids at the ω -carbon, CYP4B1 requires an unusual heme-polypeptide ester in the active site to mediate this energetically disfavored process [52].

As CYP168A1 does not catalyze the terminal ω -hydroxylation of fatty acids, it will not be involved in the production of α,ω -diacids. However, ω -1-fatty acids can be further converted to ω -1-oxo fatty acids. In *Legionella*, long chain ω -1-oxo fatty acids, also hydroxylated at the α -carbon (thus producing α -hydroxy, ω -1-oxo fatty acids), are constituents of the cell wall [53]. Also ω -1-oxo fatty acids can be further converted to ω -1-oxo dicarboxylic acids [54]. CYP168A1 does not metabolize sterols or steroids, which suggests the true substrates of CYP168A1 (if not fatty acids) are unlikely to be larger molecules. Alternatively, as in the case of CYP107H1, the fatty acids used in this study may reflect part of the true CYP168A1 substrate(s). Nevertheless, whilst the exact biological function of CYP168A1, like many other bacterial fatty acid hydroxylating CYPs, is yet to be determined, and requires further study. However, it can be hypothesized that CYP168A1 is involved in the degradation of fatty acids. Release of a high concentration of fatty acids (through high levels of phosphatidylcholine degradation) can be toxic to cells as they can cause the inhibition of enzymes involved in fatty acid degradation/ β -oxidation [55, 56]. By hydroxylating these fatty acids through an enzyme, such as CYP168A1, the toxic effect can be lessened, and fatty acids can be stored.

It may be possible to use CYP168A1 as a potential target for novel anti-*Pseudomonas* drugs. Azole antifungals are a class of inhibitor that target CYP51 enzymes, presently optimized to inhibit fungal orthologs, through the direct coordination of the imidazole N-3 or the triazole N-4 nitrogen to the CYP51 heme ferric cation as the sixth axial ligand [19]. This mode of action also means that these azole antifungals are also able to bind to the heme iron of other CYPs, such as CYP52A21 from *Candida albicans* [41], CYP124 from *Mycobacterium tuberculosis* [40] and CYP164A2 from *M. smegmatis* [57].

CYP168A1 bound miconazole with greater affinity than CYP164A2 [57] and CYP124 [40], whilst CYP168A1 bound voriconazole with similar affinity to human CYP51 [58] and with greater affinity than *M. smegmatis* CYP51 [57]. However, CYP168A1 bound azole antifungals relatively poorly compared to fungal CYP51 enzymes, which typically gave K_d values of 0.004 to 0.05 μM [58–60]. When added to reconstitution assays, where oleic acid was used as the substrate, these azoles had no effect on the catalytic activity of CYP168A1 despite the azole concentration being eight times the concentration of the enzyme used, suggesting that once the substrate is bound to CYP168A1 it is not readily displaced by the azole antifungals investigated in this study. The azole ligand binding studies were performed using pure CYP168A1 enzyme in the absence of substrate and redox partners and that azole binding properties may differ in the CYP168A1 reconstitution assays. MIC experiments with the *P. aeruginosa* strains DSMZ 22644 and ATCC 39324, grown on oleic acid, agreed with this observation as tebuconazole, miconazole and voriconazole had no inhibitory effect on growth at concentrations up to 128 $\mu\text{g ml}^{-1}$. By contrast, Tooker et al [28] reported that CYP168A1 was inhibited by ketoconazole when arachidonic acid was the substrate, resulting in a ~70% reduction in enzyme activity with a CYP168A1:ketoconazole ratio of 5 μM :10 μM , indicating screening a wider range of azole compounds may identify further CYP168A1 inhibitors. Currently available azole anti-fungal drugs would need to be redesigned and optimized to target CYP168A1 for such drugs to be considered effective inhibitors of *P. aeruginosa*.

This study has shown that the previously uncharacterized CYP168A1 from *P. aeruginosa* is involved in the sub-terminal hydroxylation of biologically relevant fatty acids. It is able to hydroxylate saturated fatty acids at both the ω -1- and ω -2-positions, but it is only able to hydroxylate unsaturated fatty acids at the ω -1-carbon.

Supporting information

S1 Fig. Mass fragmentation patterns of CYP168A1 assay metabolites. Mass fragmentation patterns for a) ω -1-hydroxy palmitic acid, diTMS, b) ω -2-hydroxy palmitic acid, diTMS, and c) ω -1-hydroxy oleic acid, diTMS are shown. TMS-derivatised fatty acids are identified by the $[M-15]^+$ fragmentation ion.

(DOCX)

Acknowledgments

We are grateful to Mr. Marcus Hull and the NMSF Mass Spectrometry Facility at Swansea University for their assistance in fatty acid analysis. We are also grateful for Dr. David D. Hughes help with the optimization of the derivatization method.

During the preparation of our manuscript, an abstract appeared with limited fatty acid metabolism data that supports our conclusions presented here. The reference for this abstract is: Tooker B, Kande, S, Work H, Lampe J. Expression and characterization of *P. aeruginosa* Cytochrome P450 CYP168A1. FASEB J. 2021; <https://doi.org/10.1096/fasebj.2021.35.S1.02588>.

Author Contributions

Conceptualization: Andrew G. S. Warrilow, Nicolae Corcionivoschi, Steven L. Kelly.

Data curation: Claire L. Price.

Formal analysis: Claire L. Price.

Funding acquisition: Andrew G. S. Warrilow, Diane E. Kelly, Steven L. Kelly.

Investigation: Claire L. Price, Nicola J. Rolley.

Methodology: Claire L. Price, Andrew G. S. Warrilow, Josie E. Parker, Vera Thoss.

Writing – original draft: Claire L. Price, Andrew G. S. Warrilow.

Writing – review & editing: Claire L. Price, Andrew G. S. Warrilow, Josie E. Parker, Diane E. Kelly, Nicolae Corcionivoschi, Steven L. Kelly.

References

1. Lyczak JB, Cannon CL, Pier GB. Lung infections associated with cystic fibrosis. Clinical microbiology reviews. 2002 Apr; 15(2):194–222. <https://doi.org/10.1128/CMR.15.2.194-222.2002> PMID: 11932230
2. Son MS, Matthews WJ, Kang Y, Nguyen DT, Hoang TT. In vivo evidence of *Pseudomonas aeruginosa* nutrient acquisition and pathogenesis in the lungs of cystic fibrosis patients. Infection and immunity. 2007; 75(11):5313–24. <https://doi.org/10.1128/IAI.01807-06> PMID: 17724070
3. Kang Y, Nguyen DT, Son MS, Hoang TT. The *Pseudomonas aeruginosa* PsrA responds to long-chain fatty acid signals to regulate the fadBA5-oxidation operon. Microbiology. 2008 Jun 1; 154(6):1584–98. <https://doi.org/10.1099/mic.0.2008/018135-0> PMID: 18524913
4. Sun Z, Kang Y, Norris MH, Troyer RM, Son MS, Schweizer HP, et al. Blocking phosphatidylcholine utilization in *Pseudomonas aeruginosa*, via mutagenesis of fatty acid, glycerol and choline degradation pathways, confirms the importance of this nutrient source *in vivo*. van Veen HW, editor. PLoS ONE. 2014 Jul 28; 9(7):e103778. <https://doi.org/10.1371/journal.pone.0103778> PMID: 25068317
5. Van Bogaert INA, Groeneboer S, Saerens K, Soetaert W. The role of cytochrome P450 monooxygenases in microbial fatty acid metabolism. FEBS Journal. 2011 Jan; 278(2):206–21. <https://doi.org/10.1111/j.1742-4658.2010.07949.x> PMID: 21156025
6. Scheller U, Zimmer T, Becher D, Schauer F, Schunck WH. Oxygenation cascade in conversion of n-alkanes to alpha,omega-dioic acids catalyzed by cytochrome P450 52A3. The Journal of biological chemistry. 1998 Dec 4; 273(49):32528–34. <https://doi.org/10.1074/jbc.273.49.32528> PMID: 9829987
7. Huang FC, Peter A, Schwab W. Expression and characterization of CYP52 genes involved in the biosynthesis of sophorolipid and alkane metabolism from *Stamerella bombicola*. Applied and Environmental Microbiology. 2014; 80(2):766–76. <https://doi.org/10.1128/AEM.02886-13> PMID: 24242247
8. Pinot F, Beisson F. Cytochrome P450 metabolizing fatty acids in plants: characterization and physiological roles. FEBS Journal. 2011 Jan; 278(2):195–205. <https://doi.org/10.1111/j.1742-4658.2010.07948.x> PMID: 21156024
9. Estabrook RW, Peterson JA, Baron J, Hildebrandt AG. The spectrophotometric measurement of turbid suspensions of cytochromes associated with drug metabolism. In: Chignell C, editor. Methods in Pharmacology, vol 2. New York: Appleton-Century-Crofts; 1972. p. 303–50. PMID: 4348512
10. Omura T, Sato R. The carbon monoxide-binding pigment of liver microsomes. The Journal of Biological Chemistry. 1964; 239:2379–85. PMID: 14209972
11. Correia MA. No Title. In: Ortiz de Montellano PR, editor. Cytochromes P450—structure, mechanism, and function. Third. Kluwer Academic / Plenum Publishers; 2005. p. 619–58.
12. Scopes RK (1974) Measurement of protein by spectrophotometry at 205 nm. Anal Biochem 59, 277–282. [https://doi.org/10.1016/0003-2697\(74\)90034-7](https://doi.org/10.1016/0003-2697(74)90034-7) PMID: 4407487
13. Schenkman JB, Jansson I. Spectral analyses of cytochromes P450. In: Phillips IR, Shephard EA, editors. Cytochrome P450 protocols. Humana Press; 2006. p. 11–8.
14. Lutz JD, Dixit V, Yeung CK, Dickmann LJ, Zelter A, Thatcher JE, et al. Expression and functional characterization of cytochrome P450 26A1, a retinoic acid hydroxylase. Biochemical Pharmacology. 2009 Jan 15; 77(2):258–68. <https://doi.org/10.1016/j.bcp.2008.10.012> PMID: 18992717
15. Luthra A, Denisov IG, Sligar SG. Spectroscopic features of cytochrome P450 reaction intermediates. Arch. Biochem. Biophys. 2011 507:26–35. <https://doi.org/10.1016/j.abb.2010.12.008> PMID: 21167809

16. Warrilow AGS, Price CL, Parker JE, Rolley NJ, Smyrniotis CJ, Hughes DD, et al. Azole antifungal sensitivity of sterol 14 α -demethylase (CYP51) and CYP5218 from *Malassezia globosa*. *Scientific Reports*. 2016 Jun 13; 6:27690. <https://doi.org/10.1038/srep27690> PMID: 27291783
17. Lamb DC, Kelly DE, Venkateswarlu K, Manning NJ, Bligh HF, Schunck WH, et al. Generation of a complete, soluble, and catalytically active sterol 14 alpha-demethylase-reductase complex. *The Journal of Biological Chemistry*. 1999; 38:8733–8.
18. Lamb DC, Skaug T, Song HL, Jackson CJ, Podust LM, Waterman MR, et al. The cytochrome P450 complement (CYPome) of *Streptomyces coelicolor* A3(2). *The Journal of Biological Chemistry*. 2002; 277:24000–5. <https://doi.org/10.1074/jbc.M111109200> PMID: 11943767
19. Jefcoate CR. Measurement of substrate and inhibitor binding to microsomal cytochrome P-450 by optical-difference spectroscopy. *Methods in Enzymology*. 1978; 52:258–79. [https://doi.org/10.1016/s0076-6879\(78\)52029-6](https://doi.org/10.1016/s0076-6879(78)52029-6) PMID: 209288
20. Bellamine A, Mangla AT, Nes WD, Waterman MR. Characterization and catalytic properties of the sterol 14alpha-demethylase from *Mycobacterium tuberculosis*. *Proceedings of the National Academy of Sciences of the United States of America*. 1999; 96(16):8937–42. <https://doi.org/10.1073/pnas.96.16.8937> PMID: 10430874
21. Hargrove TY, Wawrzak Z, Liu J, Nes WD, Waterman MR, Lepesheva GI. Substrate preferences and catalytic parameters determined by structural characteristics of sterol 14alpha-demethylase (CYP51) from *Leishmania infantum*. *The Journal of biological chemistry*. 2011 Jul 29; 286(30):26838–48. <https://doi.org/10.1074/jbc.M111.237099> PMID: 21632531
22. Cryle MJ, Schlichting I. Structural insights from a P450 carrier protein complex reveal how specificity is achieved in the P450(Biol) ACP complex. *Proceedings of the National Academy of Sciences of the United States of America*. 2008 Oct 14; 105(41):15696–701. <https://doi.org/10.1073/pnas.0805983105> PMID: 18838690
23. Sligar SG. Coupling of spin, substrate, and redox equilibria in cytochrome P450. *Biochemistry*. 1976 Nov; 15(24):5399–406. <https://doi.org/10.1021/bi00669a029> PMID: 187215
24. Bhattacharai S, Liou K, Oh T-J. Hydroxylation of long chain fatty acids by CYP147F1, a new cytochrome P450 subfamily protein from *Streptomyces peucetius*. *Archives of Biochemistry and Biophysics*. 2013 Nov; 539(1):63–9. <https://doi.org/10.1016/j.abb.2013.09.008> PMID: 24055535
25. Lepesheva GI, Virus C, Waterman MR. Conservation in the CYP51 family. Role of the B' helix/BC loop and helices F and G in enzymatic function. 2003; 42(30):9090–101. <https://doi.org/10.1021/bi034663f> PMID: 12885242
26. Locuson CW, Hutzler JM, Tracy TS. Visible spectra of type II cytochrome P450-drug complexes: evidence that “incomplete” heme coordination is common. *Drug Metabolism and Disposition*. 2007; 35 (4):614–22. <https://doi.org/10.1124/dmd.106.012609> PMID: 17251307
27. Warrilow AG, Parker JE, Kelly DE, Kelly SL. Azole affinity of sterol 14 α -demethylase (CYP51) enzymes from *Candida albicans* and *Homo sapiens*. *Antimicrobial agents and chemotherapy*. 2013 Mar; 57 (3):1352–60. <https://doi.org/10.1128/AAC.02067-12> PMID: 23274672
28. Tooker BC, Kandel SE, Work HM, Lampe JN. *Pseudomonas aeruginosa* cytochrome P450 CYP168A1 is a fatty acid hydroxylase that metabolizes arachidonic acid to the vasodilator 19-HETE [Internet]. 2021 Oct [cited 2022 Jan 10] p. 2021.10.19.465045. <https://www.biorxiv.org/content/10.1101/2021.10.19.465045v1>
29. Capyk JK, Kalscheuer R, Stewart GR, Liu J, Kwon H, Zhao R, et al. Mycobacterial cytochrome P450 125 (Cyp125) catalyzes the terminal hydroxylation of C27 steroids. *Journal of Biological Chemistry*. 2009; 284(51):35534–42. <https://doi.org/10.1074/jbc.M109.072132> PMID: 19846551
30. Williams C, Mbuyane LL, Bauer FF, Mokwena L, Divol B, Buica A. A Gas Chromatography-Mass Spectrometry Method for the Determination of Fatty Acids and Sterols in Yeast and Grape Juice. *Applied Sciences*. 2021 Jan; 11(11):5152.
31. Warrilow AGS, Martel CM, Parker JE, Melo N, Lamb DC, Nes WD, et al. Azole binding properties of *Candida albicans* sterol 14-alpha demethylase (CaCYP51). *Antimicrobial agents and chemotherapy*. 2010 Oct; 54(10):4235–45. <https://doi.org/10.1128/AAC.00587-10> PMID: 20625155
32. Eschenfeldt WH, Zhang Y, Samaha H, Stols L, Eirich LD, Wilson CR, et al. Transformation of fatty acids catalyzed by cytochrome P450 monooxygenase enzymes of *Candida tropicalis*. *Applied and environmental microbiology*. 2003 Oct; 69(10):5992–9. <https://doi.org/10.1128/AEM.69.10.5992-5999.2003> PMID: 14532054
33. Khatri Y, Hannemann F, Girhard M, Kappl R, Hutter M, Urlacher VB, et al. A natural heme-signature variant of CYP267A1 from *Sorangium cellulosum* So ce56 executes diverse ω -hydroxylation. *FEBS Journal*. 2015 Jan 1; 282(1):74–88. <https://doi.org/10.1111/febs.13104> PMID: 25302415
34. Chun Y-J, Shimada T, Sanchez-Ponce R, Martin MV, Lei L, Zhao B, et al. Electron transport pathway for a *Streptomyces* cytochrome P450: cytochrome P450 105D5-catalyzed fatty acid hydroxylation in

34. *Streptomyces coelicolor* A3(2). The Journal of biological chemistry. 2007; 282(24):17486–500. <https://doi.org/10.1074/jbc.M700863200> PMID: 17446171
35. Whitehouse CJC, Bell SG, Wong L-L, Bell SG, Wong LL, Gray HB, et al. P450_{BM3} (CYP102A1): connecting the dots. Chem Soc Rev. 2012 Jan 17; 41(3):1218–60. <https://doi.org/10.1039/c1cs15192d> PMID: 22008827
36. Green AJ, Rivers SL, Cheesman M, Reid GA, Quaroni LG, Macdonald IDG, et al. Expression, purification and characterization of cytochrome P450 Biol: a novel P450 involved in biotin synthesis in *Bacillus subtilis*. Journal of Biological Inorganic Chemistry. 2001 Jun 6; 6(5–6):523–33. <https://doi.org/10.1007/s007750100229> PMID: 11472016
37. Gustafsson MCU, Roitel O, Marshall KR, Noble MA, Chapman SK, Pessegueiro A, et al. Expression, purification, and characterization of *Bacillus subtilis* cytochromes P450 CYP102A2 and CYP102A3: flavocytochrome homologues of P450 BM3 from *Bacillus megaterium*. Biochemistry. 2004; 43(18):5474–87. <https://doi.org/10.1021/bi035904m> PMID: 15122913
38. Matsunaga I, Sumimoto T, Ueda A, Kusunose E, Ichihara K. Fatty acid-specific, regiospecific, and stereospecific hydroxylation by cytochrome P450 (CYP152B1) from *Sphingomonas paucimobilis*: substrate structure required for alpha-hydroxylation. Lipids. 2000 Apr; 35(4):365–71. <https://doi.org/10.1007/s11745-000-533-y> PMID: 10858020
39. Malca SH, Scheps D, Kühnel L, Venegas-Venegas E, Seifert A, Nestl BM, et al. Bacterial CYP153A monooxygenases for the synthesis of omega-hydroxylated fatty acids. Chemical Communications. 2012 Apr 30; 48(42):5115. <https://doi.org/10.1039/c2cc18103g> PMID: 22513828
40. Johnston JB, Kells PM, Podust LM, Ortiz de Montellano PR. Biochemical and structural characterization of CYP124: a methyl-branched lipid omega-hydroxylase from *Mycobacterium tuberculosis*. Proceedings of the National Academy of Sciences of the United States of America. 2009; 106(49):20687–92. <https://doi.org/10.1073/pnas.0907398106> PMID: 19933331
41. Kim D, Cryle MJ, De Voss JJ, Ortiz de Montellano PR. Functional expression and characterization of cytochrome P450 52A21 from *Candida albicans*. Archives of biochemistry and biophysics. 2007 Aug 15; 464(2):213–20. <https://doi.org/10.1016/j.abb.2007.02.032> PMID: 17400174
42. Kitazume T, Takaya N, Nakayama N, Shoun H. *Fusarium oxysporum* fatty-acid subterminal hydroxylase (CYP505) is a membrane-bound eukaryotic counterpart of *Bacillus megaterium* cytochrome P450BM3. The Journal of biological chemistry. 2000 Dec 15; 275(50):39734–40. <https://doi.org/10.1074/jbc.M005617200> PMID: 10995755
43. Dierks EA, Davis SC, Ortiz de Montellano PR. Glu-320 and Asp-323 are determinants of the CYP4A1 hydroxylation regiospecificity and resistance to inactivation by 1-aminobenzotriazole. Biochemistry. 1998; 37(7):1839–47. <https://doi.org/10.1021/bi972458s> PMID: 9485309
44. Hoch U, Ortiz De Montellano PR. Covalently linked heme in cytochrome P4504a fatty acid hydroxylases. The Journal of biological chemistry. 2001 Apr 6; 276(14):11339–46. <https://doi.org/10.1074/jbc.M009969200> PMID: 11139583
45. Cryle MJ, Matovic NJ, De Voss JJ. Products of cytochrome P450 Biol (CYP107H1)-catalyzed oxidation of fatty acids. Organic Letters. 2003; 5(18):3341–4. <https://doi.org/10.1021/o1035254e> PMID: 12943422
46. Capdevila JH, Wei S, Helvig C, Falck JR, Belosludtsev Y, Truan G, et al. The highly stereoselective oxidation of polyunsaturated fatty acids by cytochrome P450BM-3. The Journal of biological chemistry. 1996; 271(37):22663–71. <https://doi.org/10.1074/jbc.271.37.22663> PMID: 8798438
47. Lim Y-R, Eun C-Y, Park H-G, Han S, Han J-S, Cho KS, et al. Regioselective oxidation of lauric acid by CYP119, an orphan cytochrome P450 from *Sulfolobus acidocaldarius*. Journal of microbiology and biotechnology. 2010 Mar; 20(3):574–8. PMID: 20372030
48. Lasker JM, Chen WB, Wolf I, Bloswick BP, Wilson PD, Powell PK. Formation of 20-hydroxyeicosatetraenoic acid, a vasoactive and natriuretic eicosanoid, in human kidney. Role of Cyp4F2 and Cyp4A11. The Journal of biological chemistry. 2000 Feb 11; 275(6):4118–26. <https://doi.org/10.1074/jbc.275.6.4118> PMID: 10660572
49. Harmon SD, Fang X, Kaduce TL, Hu S, Raj Gopal V, Falck JR, et al. Oxygenation of ω-3 fatty acids by human cytochrome P450 4F3B: effect on 20-hydroxyeicosatetraenoic acid production. Prostaglandins, Leukotrienes and Essential Fatty Acids. 2006 Sep; 75(3):169–77. <https://doi.org/10.1016/j.plefa.2006.05.005> PMID: 16820285
50. Tang Z, Salamanca-Pinzón SG, Wu Z-L, Xiao Y, Guengerich FP. Human cytochrome P450 4F11: heterologous expression in bacteria, purification, and characterization of catalytic function. Archives of Biochemistry and Biophysics. 2010 Feb 1; 494(1):86–93. <https://doi.org/10.1016/j.abb.2009.11.017> PMID: 19932081
51. Nakano M, Kelly EJ, Rettie AE. Expression and characterization of CYP4V2 as a fatty acid omega-hydroxylase. Drug metabolism and disposition: the biological fate of chemicals. 2009 Nov; 37(11):2119–22. <https://doi.org/10.1124/dmd.109.028530> PMID: 19661213

52. Scott EE. ω - versus (ω -1)-hydroxylation: cytochrome P450 4B1 sterics make the call. *The Journal of biological chemistry*. 2017 Mar 31; 292(13):5622–3. <https://doi.org/10.1074/jbc.H117.775494> PMID: 28363936
53. Sonesson A, Moll H, Jantzen E, Zähringer U. Long-chain alpha-hydroxy-(omega-1)-oxo fatty acids and alpha-hydroxy-1,omega-dioic fatty acids are cell wall constituents of *Legionella* (*L. jordanis*, *L. maceachernii* and *L. micdadei*). *FEMS microbiology letters*. 1993; 106(3):315–20. <https://doi.org/10.1111/j.1574-6968.1993.tb05982.x> PMID: 8454196
54. Kundu RK, Getz GS, Tonsgard JH. Induction of (omega-1)-oxidation of monocarboxylic acids by acetyl-salicylic acid. *Journal of lipid research*. 1993 Jul; 34(7):1187–99. PMID: 8371066
55. Parsons JB, Yao J, Frank MW, Jackson P, Rock CO. Membrane Disruption by Antimicrobial Fatty Acids Releases Low-Molecular-Weight Proteins from *Staphylococcus aureus*. *Journal of Bacteriology*. 2012 Oct 1; 194(19):5294–304. <https://doi.org/10.1128/JB.00743-12> PMID: 22843840
56. Urlacher VB, Eiben S. Cytochrome P450 monooxygenases: perspectives for synthetic application. *Trends in Biotechnology*. 2006 Jul 1; 24(7):324–30. <https://doi.org/10.1016/j.tibtech.2006.05.002> PMID: 16759725
57. Warrilow AGS, Jackson CJ, Parker JE, Marczylo TH, Kelly DE, Lamb DC, et al. Identification, characterization, and azole-binding properties of *Mycobacterium smegmatis* CYP164A2, a homolog of ML2088, the sole cytochrome P450 gene of *Mycobacterium leprae*. *Antimicrobial Agents and Chemotherapy*. 2009 Mar 1; 53(3):1157–64. <https://doi.org/10.1128/AAC.01237-08> PMID: 19075057
58. Warrilow AGS, Parker JE, Price CL, Nes WD, Garvey EP, Hoekstra WJ, et al. The Investigational Drug VT-1129 Is a Highly Potent Inhibitor of *Cryptococcus* Species CYP51 but Only Weakly Inhibits the Human Enzyme. *Antimicrobial agents and chemotherapy*. 2016 Aug; 60(8):4530–8. <https://doi.org/10.1128/AAC.00349-16> PMID: 27161631
59. Parker JE, Warrilow AGS, Cools HJ, Martel CM, Nes WD, Fraaije BA, et al. Mechanism of binding of prothioconazole to *Mycosphaerella graminicola* CYP51 differs from that of other azole antifungals. *Antimicrobial Agents and Chemotherapy*. 2011; 77(4):1460–5. <https://doi.org/10.1128/AEM.01332-10> PMID: 21169436
60. Warrilow AGS, Melo N, Martel CM, Parker JE, Nes WD, Kelly SL, et al. Expression, purification, and characterization of *Aspergillus fumigatus* sterol 14-demethylase (CYP51) isoenzymes A and B. *Antimicrobial Agents and Chemotherapy*. 2010 Oct 1; 54(10):4225–34. <https://doi.org/10.1128/AAC.00316-10> PMID: 20660663
61. Copeland RA. Evaluation of enzyme inhibitors in drug discovery: a guide for medicinal chemists and pharmacologists. Wiley-Interscience, New York, NY; 2005. 178–213 p.